Anti-atherosclerotic effects of genistein in preventing ox-low-density lipoprotein-induced smooth muscle-derived foam cell formation via inhibiting *SRC* expression and L-Ca channel currents

Wei Zhang[1], Liming Zhang[1], Xiaosi Zhang[2]

[1]Department of Neurology, The First Affiliated Hospital of Harbin Medical University, Harbin, China; [2]Metro-Medic Clinic, Montreal, Quebec, Canada

Contributions: (I) Conception and design: W Zhang; (II) Administrative support: L Zhang; (III) Provision of study materials or patients: L Zhang; (IV) Collection and assembly of data: W Zhang; (V) Data analysis and interpretation: W Zhang, X Zhang; (VI) Manuscript writing: All authors; (VII) Final approval of manuscript: All authors.

Correspondence to: Liming Zhang. Department of Neurology, The First Affiliated Hospital of Harbin Medical University, 23 Youzheng Street, Nangang District, Harbin 150001, Heilongjiang, China. Email: zhangfx0001@sina.com; Xiaosi Zhang. Metro-Medic Clinic, Suite 100, 1538 Sherbrooke West Street, Montreal, Quebec, Canada. Email: zxiaosi686@163.com.

Background: Atherosclerosis (AS) is associated with inflammation and abnormal proliferation and migration of vascular smooth muscle cells (VSMCs). Genistein may curtail the migration of VSMCs. Therefore, explorations are required to determine the molecular mechanism of genistein in AS. In this context, animal and cell models were developed to ascertain mechanisms of genistein in AS by modulating VSMC activities.

Methods: Genistein treatment and ectopic expression of lectin-like oxidized LDL receptor-1 (*LOX-1*) were conducted in high-fat diet-induced AS rats, followed by analyses of atherosclerotic plaque lesion areas and lipid deposition using Oil Red O and hematoxylin and eosin (HE) staining. The isolated VSMCs were stimulated with oxidized low-density lipoprotein (ox-LDL). Following genistein treatment combined with gain- and loss-of-function experiments in ox-LDL-exposed VSMCs, viability, migration, intracellular lipid deposition, intracellular cholesterol content, and L-type calcium (L-Ca) channel currents were assessed using Cell Counting Kit-8 (CCK-8), scratch test, Oil Red O staining, enzymatic colorimetry, and patch-clamp experiments, respectively. Western blot analysis was performed to evaluate the protein expression of *SRC* proto-oncogene, non-receptor tyrosine kinase (*SRC*), calcium voltage-gated channel subunit alpha1 C (*CACNA1C*), and *LOX-1*.

Results: Genistein treatment counteracted upregulated *SRC* phosphorylation, *CACNA1C* and *LOX-1* expression, and L-Ca channel currents in aortic tissues of AS rats and ox-LDL-exposed VSMCs. Genistein deceased L-Ca channel currents by downregulating *SRC*, and *SRC* augmented *LOX-1* expression by acting on the L-Ca channel subunit *CACNA1C*. The ox-LDL-induced VSMC proliferation, migration, and foaming of VSMCs were reduced by genistein treatment, silencing *SRC*, *CACNA1C*, or *LOX-1*, or suppressing L-Ca channels. Genistein treatment diminished atherosclerotic plaque lesion formation and lipid deposition, and these results were annulled by upregulating *LOX-1*.

Conclusions: Collectively, genistein might block the *SRC/CACNA1C/LOX-1* axis to impede ox-LDL-induced VSMC proliferation, migration, and foaming and alleviate AS formation.

Keywords: Atherosclerosis; vascular smooth muscle cell; genistein; *SRC*; L-type calcium channels

Introduction

As a chronic inflammatory disorder of large and medium-sized arteries, atherosclerosis (AS) contributes to stroke, peripheral vascular disease, and ischemic heart disease, collectively named cardiovascular diseases (CVDs) (1). The profile of risks carried by low-density lipoprotein (LDL) cholesterol, blood pressure and smoking has been shifting to triglyceride-rich lipoproteins and LDL as contributors in AS (2). The oxidized low-density lipoprotein (ox-LDL) is abundant in atherosclerotic lesions showing proinflammatory and immune-stimulatory properties, which contributes to development of AS, plaque rupture, and CVDs (3). Atherosclerotic lesions are majorly characterized by lipid deposition in some arteries, accompanied by smooth muscle cell (SMC) and fibrous matrix proliferation, which gradually progresses to atherosclerotic plaque formation (4). Foam cells have been implicated in all stages of atherosclerotic lesion development, a large part of which originate from vascular SMCs (VSMCs) (5). Moreover, the rapid deposition of oxidized lipids, including ox-LDL, in the circulation results in migration and foaming necrosis of a large amount of VSMCs, thus facilitating AS formation (6,7). Of note, the involvement of L-type calcium (L-Ca) channels has been revealed in VSMC migration (8). Therefore, there is an ongoing urgent need to ascertain the molecular mechanism behind L-Ca channels and VSMC proliferation, migration, and foaming in AS for the exploration of promising targets for AS treatment.

As a biologically active isoflavone existing in soy, genistein orchestrates multiple pathophysiologic pathways linked to cancer, metabolic syndrome, and obesity (9). A prior study elaborated the atheroprotective effects of genistein in apolipoprotein E-deficient rats (10). Genistein has also been reported to decrease VSMC proliferation caused by ox-LDL (11). Of note, the study by Ono *et al.* manifested that genistein restrained *SRC* proto-oncogene, non-receptor tyrosine kinase (*SRC*)-induced cell proliferation in human gallbladder carcinoma (12). The *SRC* protein belongs to the *SRC* family of protein tyrosine kinases that are present in all mammalian cells and involved in numerous cell processes like differentiation, proliferation, and migration (13). The implication of *SRC* has been displayed in foam cell formation in macrophages and lesion development in AS (14). Furthermore, *SRC* could activate L-Ca channels in immature mouse cardiomyocytes (15). Meanwhile, calcium voltage-gated channel subunit alpha1 C (*CACNA1C*)

encodes Ca1.2 of L-Ca channels, which participates in the process of AS (16,17). A study uncovered that *CACNA1C* was related to the upregulation of lectin-like oxidized LDL receptor-1 (*LOX-1*) during the differentiation and activation of macrophages (18). Notably, a recent study showed that *LOX-1* was upregulated in AS rats, which accelerated ox-LDL uptake in the aorta of the rats (19). Still, the molecular causes leading to VSMC proliferation, migration, and foaming are poorly understood, and effective treatments for AS are slow to emerge. There remain many unanswered questions in regards to the downstream mechanistic actions of genistein and the involvement of L-Ca channel currents in the biological characteristics of VSMCs. These previously uncharacterized questions are considered in the present study.

In this context, we speculated that genistein might control AS progression via the *SRC/CACNA1C/LOX-1* axis. Therefore, an AS rat model was established to identify *SRC*, *CACNA1C*, and *LOX-1* expression after genistein treatment, and a cell model was developed on VSMCs using ox-LDL to further dissect their role in AS by measuring the proliferation, migration, and foaming of VSMCs. We present the following article in accordance with the ARRIVE reporting checklist (available at https://atm.amegroups.com/article/view/10.21037/atm-22-2113/rc).

Methods

AS rat model establishment

A total of 56 12-week-old specific-pathogen-free (SPF) Sprague-Dawley (SD) rats were purchased from the Laboratory Animal Center, Harbin Medical University (Heilongjiang, China). Rats were individually housed in an SPF animal laboratory with 60–65% humidity at 22–25 ℃. The experimentations were started after 1-week of acclimatization. The health status of rats was observed prior to the experiments. Animal experiments were performed under a project license (No. 2021086) granted by Animal Ethical Care Committee of the First Affiliated Hospital of Harbin Medical University, in compliance with institutional guidelines for the care and use of animals. A protocol was prepared before the study without registration.

We randomly selected 8 rats from the 56 to undergo sham-operation, and fed them with conventional chow for 12 weeks. The remaining rats were fed with a high-fat diet (HFD; D12108C, Biopike, Beijing, China) containing

1.25% cholesterol, 10% fat, and 0.1% propylthiouracil for 12 weeks to induce the AS model.

The untreated AS rats served as the AS group, and the remaining AS rats were treated with dimethyl sulfoxide (DMSO), genistein, DMSO+ overexpression (oe)-negative control (NC), genistein + oe-NC, and genistein + oe-*LOX-1* (8 rats/group). For the genistein treatment, rats were fed with HFD and gavaged daily with 45 mg/kg genistein or an equivalent volume of DMSO (abs47048069; Absin Bioscience Inc., Shanghai, China) as control. Besides, lentivirus-based *LOX-1* overexpression vectors were constructed with a titer of 1×10^8 TU/mL. While being fed with the HFD, rats were injected with 0.1 mL lentiviruses via the tail vein every 3 days. After 12 weeks, rats were euthanized using the carbon dioxide asphyxiation method, followed by collection of aortic tissues for tissue staining to observe atherosclerotic plaques, lesion areas, and lipid deposition.

Oil Red O staining

Following fixation of slides of cells, aorta, or aortic root using 4% formaldehyde, they were stained with Oil Red O solution (01391, Sigma-Aldrich, St. Louis, MO, USA) for 30 minutes. Samples were then rinsed with 75% ethanol for 5 minutes and with phosphate-buffered saline (PBS), followed by immediate imaging. Oil Red O-positive cells were photographed using an optical microscope (Nikon, Tokyo, Japan).

Hematoxylin and eosin staining

Aortic tissues were attained at week 12 after modeling, fixed in 4% formaldehyde, and dehydrated in gradient alcohol. Following 2 xylene washes, aortic tissue sections were dewaxed, and hydrated, followed by hematoxylin and eosin (HE) staining according to the manuals of an HE staining kit (PT001; Bogoo, Shanghai, China). In detail, after 10 minutes of staining in hematoxylin at room temperature, the sections were hydrolyzed in 1% hydrochloric acid solution for 20 seconds, and then treated in 1% ammonia solution for 30 seconds. Subsequent to 3 minutes of eosin staining of the sections, the morphology of aortic atherosclerotic lesions was observed under the optical microscope.

Isolation and identification of VSMCs

Aortas were collected, and arterial fat and connective tissue were carefully isolated. The arteries were then cut into blocks of 1 mm in length. These sections were incubated for 20–25 minutes at 37 ℃ in a solution containing 1.5 mg/mL papain, 1.5 mg/mL threitol, and 1.5 mg/mL bovine serum albumin (BSA), followed by 6–10 minutes of treatment with 1.0 mg/mL collagenase, 1.5 mg/mL hyaluronidase, and 1.5 mg/mL BSA. After that, SMCs were separated by gentle grinding with a pipette. Cells were maintained in Dulbecco's Modified Eagle Medium (DMEM) comprising 20% fetal bovine serum (FBS) and 100 U/mL streptomycin/penicillin. Finally, immunofluorescence detection of α-smooth muscle actin (α-SMA) was conducted to identify VSMCs using primary rabbit antibody against α-SMA (1:500, Ab124964; Abcam, Cambridge, UK) and Alexa Fluor® 488-labeled secondary goat anti-mouse immunoglobulin G (IgG) (H+L) antibody (1:800, Ab150081; Abcam, UK).

Papain, threitol, BSA, collagenase, hyaluronidase, FBS, and streptomycin/penicillin were purchased from Solarbio (Beijing, China; G8430, D8220, A8010, C8140, H8030, S9030, and P1400, respectively).

In vitro cell model of ox-LDL-exposed VSMCs

The isolated VSMCs were stimulated with ox-LDL to develop *in vitro* cell model. The VSMCs received no treatment and served as controls, whilst ox-LDL-exposed VSMCs were untreated or treated with DMSO, genistein, BayK8644, nifedipine, genistein + BayK8644, short hairpin RNA (sh)-NC, sh-*SRC*, DMSO + oe-NC, genistein + oe-NC, genistein + oe-*SRC*, genistein + oe-*LOX-1*, oe-NC + sh-NC, oe-*SRC* + sh-NC, oe-*SRC* + sh-*CACNA1C*, sh-*CACNA1C* + oe-NC, or sh-*CACNA1C* + oe-*LOX-1*.

For the ox-LDL exposure, VSMCs were stimulated with 75 μg/mL of ox-LDL for 72 hours. The VSMCs were treated with 50 μmol/L genistein, 30 μmol/L BayK8644 (the L-Ca channel activator), and 50 μmol/L nifedipine (the L-Ca channel blocker) (HY-10588 and HY-B0284, respectively; MedChemExpress, Monmouth Junction, NJ, USA) 6 hours before ox-LDL exposure. Cells were grouped by liposome transfection with shRNA primers (sh-*SRC*, GCAAGATCACTAGACGGGAAT and sh-*CACNA1C*, CGCAGTCAAGTCTAATGTCTT) and pCMV6-AC-GFP (the overexpression vector, FH1215; Feng Hui Biotechnology Co., Ltd., Hunan, China). Transfection was performed using a lipofectamine 2000 kit (11668019, Thermo Fisher Scientific, Waltham, MA, USA). After 6 hours transfection, the medium was replaced with complete medium for 48 hours incubation. The cells were

harvested to detect the transfection efficiency and utilized for subsequent experiments.

Western blot analysis

Total tissue or cellular protein was extracted using radio-immunoprecipitation assay (RIPA) lysis containing phenylmethylsulfonyl fluoride (P0013C; Beyotime, Shanghai, China), followed by 30 minutes incubation on ice and 10 minutes centrifugation at 4 ℃ and 8,000 g. Following the collection of the supernatant, the total protein concentration was measured with a bicinchoninic acid (BCA) kit. After 50 μg proteins were dissolved in 2× sodium dodecyl sulfate (SDS) loading buffer, each sample was subjected to SDS-polyacrylamide gel electrophoresis (SDS-PAGE) and electro-blotted to polyvinylidene fluoride (PVDF) membranes. Afterward, the membranes underwent 1 hour blocking with 5% skimmed milk powder at room temperature and probed with diluted primary antibodies (Abcam, UK) against *SRC* (1:1,000, ab133283, rabbit), phosphorylation (p)-*SRC* (1:5,000, ab185617, rabbit), *CACNA1C* (1:1,200, ab84814, mouse), *LOX-1* (1:1,000, ab214427, rabbit), and glyceraldehyde-3-phosphate dehydrogenase (GAPDH; ab9485, 1:2,500, loading control) overnight at 4 ℃. Next, the membranes were re-probed with horseradish peroxidase (HRP)-tagged secondary antibodies (Abcam, UK) against goat anti-rabbit IgG H&L (ab97051, 1:2,000) and goat anti-mouse IgG (H&L) (ab6789, 1:2,000) for 1 hour. The blots were visualized by enhanced chemiluminescence (ECL) kit (abs920, Absin) and photographed with a Bio-Rad image analysis system (Bio-Rad Laboratories, Hercules, CA, USA), followed by analysis with Quantity One v4.6.2 software (Bio-Rad, USA).

Patch-clamp experiments

Electrode solution (mM) comprised CsCl 110, Na2 phosphocreatine 20, egtazic acid (EGTA) 10, Na2ATP 5, MgCl2 5, NaGTP 0.2, and HEPES 10, with solution PH adjusted to 7.3 by CsOH. Extracellular bath solution (mM) was comprised of NaCl 135, BaCl$_2$ 10, TEA-Cl 10, HEPES 10, CsCl 5, and Glucose 10, with solution PH adjusted to 7.4 by CsOH. Experiments were carried out at room temperature. The glass microelectrode was made by 3–4 pulls of a microelectrode micropipette puller (Model P-97; Sutter Instrument, Novato, CA, USA) on the day of the experiment which was used with a resistance range of 4–7 MΩ. The cell membrane capacitance was in the range

of 12.15±3.41 pF (n=96), with an access resistance >2 GΩ. The current at 10 mV was depolarized from –50 to +40 mV with a step of 500 ms, and current was recorded with a sampling frequency of 10 kHz at a holding potential of –70 mV. In this study, the whole-cell L-Ca current was recorded using a Axopatch 200B amplifier (Axon Instruments, Burlingame, CA, USA), Axon pCLAMP9.2 software, and digidata1322A interface (Axon Instruments, USA).

Cell Counting Kit-8 (CCK-8)

A CCK-8 kit (CK04; Dojindo Laboratories, Kumamoto, Japan) was applied for measurement of cell viability. Logarithmic growing cells were seeded at 1×10^4 per well in a 96-well plate for 24 hours. Cells were then grouped, and 10 μL CCK-8 reagents were added at 0, 24, 48, and 72 hours after grouping, and incubated at 37 ℃ for 3 hours. The absorbance values of each well at 450 nm were measured on a microplate reader, and the values were proportional to the number of cells proliferating in the culture medium. The growth curve was plotted.

Scratch test

The concentration of the cells was adjusted to 1×10^6 cells/mL with DMEM, and the cells were routinely cultured in 10% DMEM encompassing FBS until cell monolayers formed. The pipette tip was adopted to scratch along the bottom of the culture plate in a "1" shape, and the relative distance of the scratch area was recorded under a microscope. Then, the cells were washed with serum-free medium, followed by 24 hours of routine incubation. The cells were observed and photographed under an inverted microscope (Nikon, Japan) to assess the relative distance of cell migration to the wounded area. The actual cell migration distance was calculated as per the distance from the original cell injury area.

Immunofluorescence

The VSMCs were treated with PBS with the cell concentration adjusted to 1×10^6 cells/mL. Cells were supplemented with 20 μg/mL 1,1'-dioctadecyl-3,3,3',3'-tetramethylindocarbocyanine perchlorate (Dil) cell membrane-labeled ox-LDL (Dil-ox-LDL) fluorescent dye for 4 hours incubation in a 37 ℃ incubator with 5% CO$_2$ and saturation humidity. Following incubation, the intensity of Dil-ox-LDL fluorescence staining in cells was

observed under an inverted fluorescence microscope (BX50; Olympus, Japan).

Enzymatic colorimetry

The cells were attained, and 1×10^6 cells were extracted with 200 µL cholesterol extract (trichloromethane: isopropanol: NP40 =7:11:0.1), followed by the determination of the cholesterol concentration. The remaining precipitates were lysed with 200 µL RIPA lysis buffer. Afterward, the protein concentration was estimated using the Lowry method, and the amount of cholesterol per mg of protein (µg/mg) was calculated.

Statistical analysis

All statistical analyses of the data were implemented using the software SPSS 21.0 (IBM Corp., Armonk, NY, USA). The measurement data were summarized as mean ± standard deviation and tested for normal distribution and homogeneity of variance. If the data conformed to normal distribution and homogeneity of variance, unpaired t-tests were utilized to compare data between the 2 groups. One-way analysis of variance (ANOVA) or repeated measures ANOVA was employed to compare data among multiple groups, followed by Tukey's post-hoc test. A P value <0.05 indicated that the differences were statistically significant.

Results

Genistein alleviated AS in rats and inhibited ox-LDL-induced proliferation, migration, and foaming of VSMCs in vitro

To investigate the molecular mechanisms by which genistein affected AS, a rat model of AS was established. The results of Oil Red O staining and HE staining (*Figure 1A-1C*) showed that the atherosclerotic plaque lesion area and lipid deposition were significantly increased in rats after AS modeling, and that when AS rats were treated with genistein, the atherosclerotic plaque lesion area and lipid deposition were obviously decreased. This indicated that genistein could alleviate AS in rats.

Rat VSMCs were isolated to develop an *in vitro* cell model. The VSMCs were identified by immunofluorescence detection of α-SMA in cells. The results (*Figure 1D*) displayed that VSMCs had green fluorescence, indicating their successful extraction. Next, VSMCs were stimulated

with ox-LDL to develop an *in vitro* cell model. As reflected by the results of CCK-8 and scratch test (*Figure 1E,1F*, Figure S1A), ox-LDL strikingly enhanced cell viability and migration in VSMCs, whilst treatment with genistein markedly reduced the viability and migration of ox-LDL-exposed VSMCs. Uptake of large amounts of fat by VSMCs leads to cholesterol accumulation, which foams the cells, causing AS (20). Oil Red O staining (*Figure 1G*) demonstrated a dramatic increase of intracellular lipid particles in ox-LDL-exposed VSMCs and noticeable decline of intracellular lipid particles inox-LDL-exposed VSMCs following genistein treatment. Enzymatic colorimetry results (*Figure 1H*) documented that intracellular cholesterol content was substantially elevated in VSMCs by ox-LDL exposure, and that intracellular cholesterol content was conspicuously diminished in ox-LDL-exposed VSMCs after genistein treatment. These data suggested that genistein could inhibit ox-LDL-induced proliferation, migration, and foaming of VSMCs.

Genistein restrained ox-LDL-induced proliferation, migration, and foaming of VSMCs by decreasing L-Ca channel currents

Research has illustrated that genistein curtails L-Ca channels (21). To explore the influence of genistein on L-Ca channels, patch-clamp experiments were performed to detect L-Ca channel currents in VSMCs, which displayed that L-Ca channel currents were evidently augmented in VSMCs by ox-LDL exposure, which was nullified by genistein treatment (*Figure 2A*). Treatment of VSMCs with the L-Ca channel activator BayK8644 and blocker nifedipine revealed that cellular L-Ca channel currents were clearly increased after treatment with BayK8644 but decreased after treatment with nifedipine in ox-LDL-exposed VSMCs. Moreover, BayK8644 reversed the reduction of L-Ca channel currents by genistein in ox-LDL-exposed VSMCs (*Figure 2B*). Collectively, genistein suppressed ox-LDL-induced L-Ca channel currents in VSMC-derived foam cells.

We further ascertained the effect of genistein on ox-LDL-exposed VSMC activities through inhibition of L-Ca channel currents. With respect to CCK-8 and scratch test results (*Figure 2C,2D*, Figure S1B), BayK8644 considerably enhanced but nifedipine prominently reduced ox-LDL-exposed VSMC viability and migration, and then BayK8644 annulled the decline of ox-LDL-exposed VSMC viability and migration induced genistein. As for the results of Oil
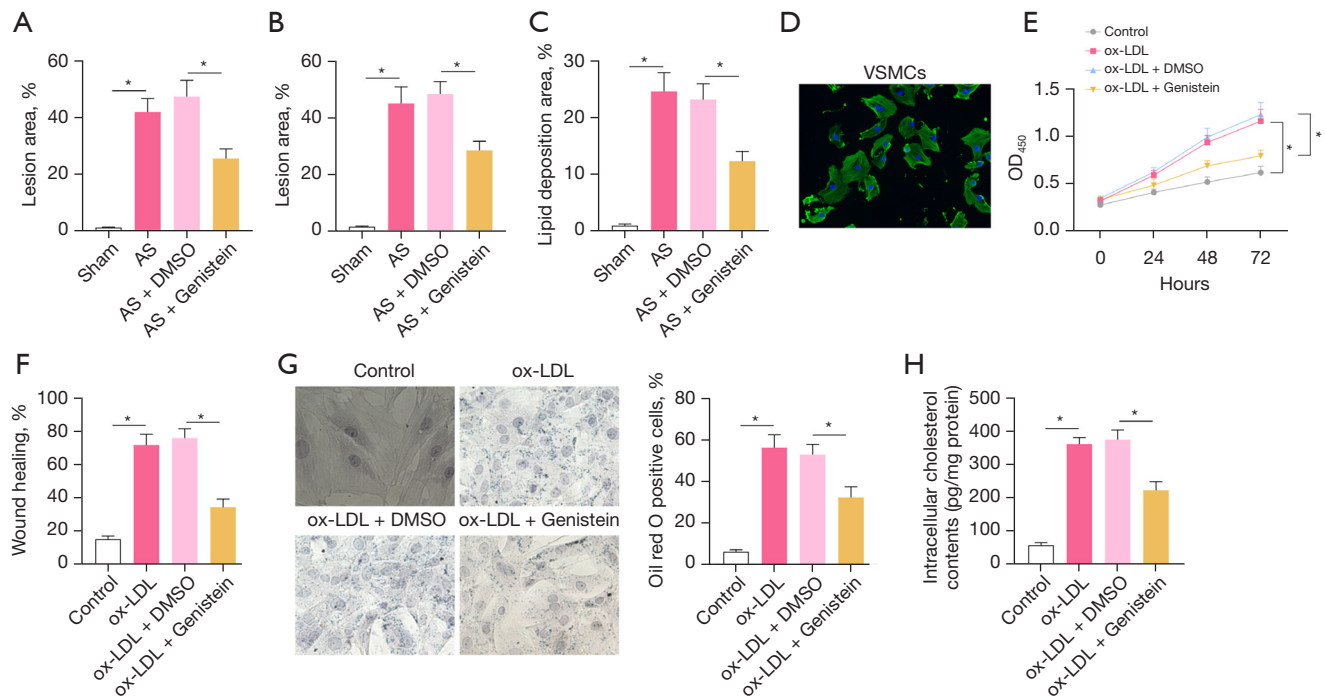
Figure 1 Genistein attenuates AS in rats and represses ox-LDL-induced VSMC proliferation, migration, and foaming. Rats underwent sham-operation as controls, and AS rats were untreated or treated with DMSO or genistein. (A) Oil Red O staining analysis of whole aortic atherosclerotic lesion area (8 rats per group). (B) HE staining analysis of aortic root lesion area (8 rats per group). (C) Oil Red O staining detection of percentage of aortic root lipids (8 rats per group). (D) VSMC identification. VSMCs received no treatment served as controls, whereas ox-LDL-induced VSMCs were untreated or treated with DMSO or genistein, (observed at 100 μm). (E) CCK-8 detection of VSMC viability. (F) Scratch test to detect VSMC migration. (G) Oil Red O staining to analyze lipid deposition in VSMCs. Control (400 μm), ox-LDL (200 μm), ox-LDL + DMSO (200 μm), ox-LDL + genistein (200 μm). (H) Enzymatic colorimetry to determine cholesterol content in VSMCs. *P<0.05. The cell experiments were repeated 3 times independently. AS, atherosclerosis; ox-LDL, oxidized low-density lipoprotein; VSMC, vascular smooth muscle cell; DMSO, dimethyl sulfoxide; HE, hematoxylin and eosin; CCK-8, Cell Counting Kit-8.

Red O staining and enzymatic colorimetry (*Figure 2E,2F*), BayK8644 significantly increased intracellular lipid particles and cholesterol content in ox-LDL-exposed VSMCs, which was contrary after nifedipine treatment. BayK8644 abrogated the repressive impact of genistein on intracellular lipid particles and cholesterol content in ox-LDL-exposed VSMCs.

Conclusively, genistein could subdue ox-LDL-induced proliferation, migration, and foaming of VSMCs via the reduction of L-Ca channel currents.

Genistein suppressed ox-LDL-exposed VSMC proliferation, migration, and foaming by diminishing SRC activity

As tyrosine kinases, *SRC* family kinases have been indicated to assume a role in the atherosclerotic process (22). Since

genistein is a tyrosine kinase inhibitor, we hypothesized that it could impact the activities of ox-LDL-induced VSMCs by repressing *SRC* activity. Western blot analysis results (*Figure 3A,3B*) exhibited that *SRC* phosphorylation level was significantly enhanced in the aortic tissues of rats by AS modeling, which was counteracted by genistein treatment. The *SRC* phosphorylation level was obviously elevated in VSMCs by ox-LDL exposure, which was negated after genistein treatment. This suggested that *SRC* was hyperphosphorylated in atherosclerotic tissues and that genistein could restrict *SRC* activity in AS.

To dissect the influence of genistein on activities of ox-LDL-induced VSMCs by downregulating *SRC*, ox-LDL-induced VSMCs were treated with genistein, sh-*SRC*, or oe-*SRC*. Western blot analysis results (*Figure 3C*) documented appreciable reduction of *SRC* phosphorylation level in ox-
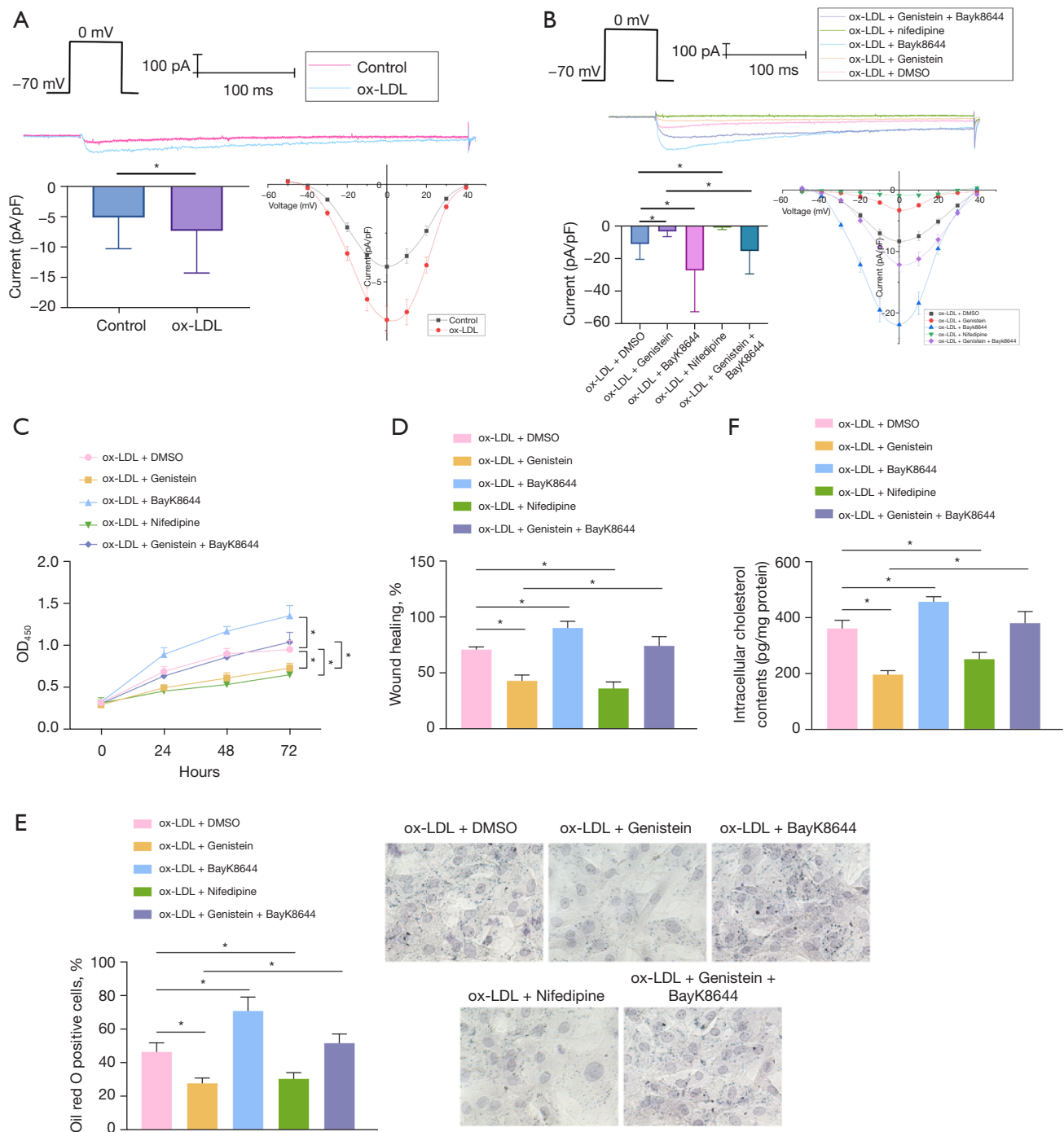
Figure 2 Genistein decreases proliferation, migration, and foaming of ox-LDL-induced VSMCs through inhibiting L-Ca channel currents. (A) Patch-clamp experiments to measure L-Ca channel currents in VSMCs after ox-LDL exposure. ox-LDL-induced VSMCs were treated with DMSO, genistein, BayK8644, nifedipine, or genistein + BayK8644. (B) Patch-clamp experiments to determine L-Ca channel currents in VSMCs. (C) CCK-8 detection of viability of VSMCs. (D) Scratch test to examine migration of VSMCs. (E) Oil Red O staining analysis of lipid deposition in VSMCs (all observed at 200 μm). (F) Enzymatic colorimetry assessment of cholesterol content in VSMCs. *P<0.05. The cell experiments were repeated 3 times independently. ox-LDL, oxidized low-density lipoprotein; VSMC, vascular smooth muscle cell; DMSO, dimethyl sulfoxide; CCK-8, Cell Counting Kit-8.
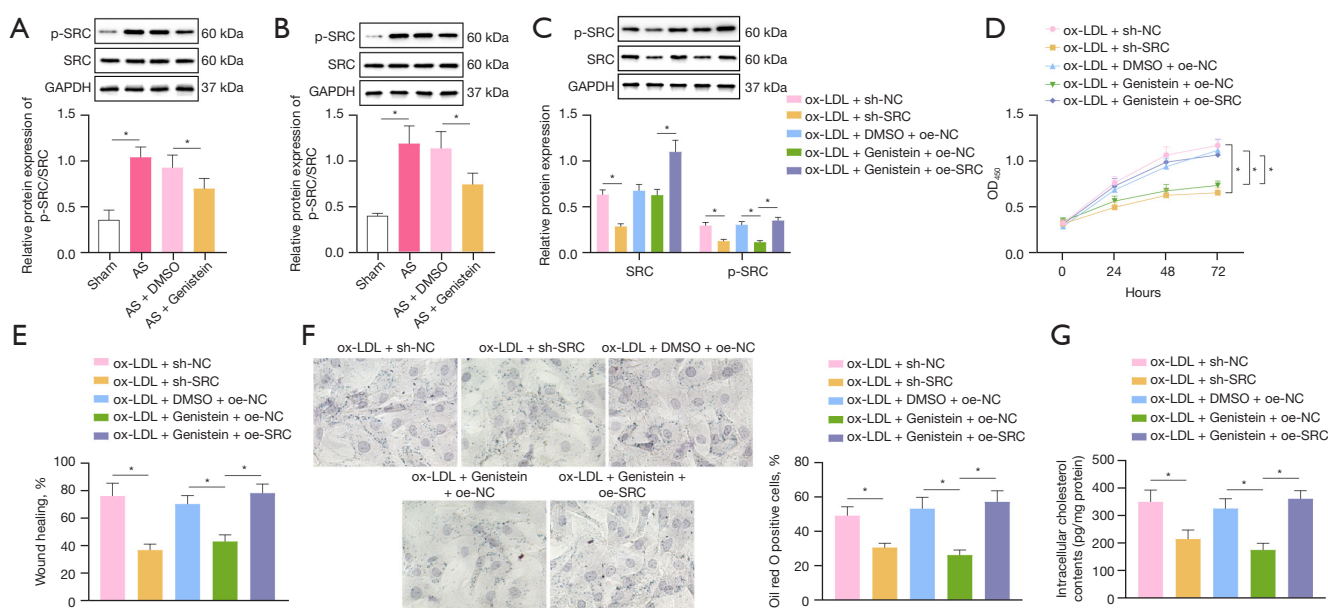
Figure 3 Genistein-mediated downregulation of *SRC* decreases ox-LDL-induced proliferation, migration, and foaming of VSMCs. (A) Western blot analysis of *SRC* phosphorylation level in aortic tissue of rats after AS modeling and genistein treatment (8 rats per group). (B) Western blot analysis of *SRC* phosphorylation level in VSMCs after ox-LDL exposure and genistein treatment. (C) Western blot analysis of *SRC* phosphorylation level in ox-LDL-induced VSMCs in response to sh-*SRC*, genistein alone or combined with oe-*SRC*. (D) Viability of ox-LDL-induced VSMCs in response to sh-*SRC*, genistein alone or combined with oe-*SRC* determined by CCK-8 assay. (E) Migration of ox-LDL-induced VSMCs in response to sh-*SRC*, genistein alone or combined with oe-*SRC* assessed by scratch test. (F) Oil Red O staining to evaluate lipid deposition of ox-LDL-induced VSMCs in response to sh-*SRC*, genistein alone or combined with oe-*SRC* (all observed at 200 µm). (G) Enzymatic colorimetry to test the cholesterol content of ox-LDL-induced VSMCs in response to sh-*SRC*, genistein alone or combined with oe-*SRC*. *P<0.05. The cell experiments were repeated 3 times independently. AS, atherosclerosis; ox-LDL, oxidized low-density lipoprotein; VSMC, vascular smooth muscle cell; DMSO, dimethyl sulfoxide; CCK-8, Cell Counting Kit-8.

LDL-induced VSMCs after silencing *SRC* or treatment with genistein. Furthermore, overexpression of *SRC* neutralized the inhibitory effect of genistein on *SRC* phosphorylation level. Besides, CCK-8 and scratch test (*Figure 3D,3E*, Figure S1C) depicted that silencing *SRC* or treatment with genistein observably lowered ox-LDL-induced VSMC proliferative and migratory capacity. Overexpression of *SRC* counterweighed the suppressive impacts of genistein on ox-LDL-induced VSMC proliferative and migratory capacity. The results of Oil Red O staining and enzymatic colorimetry (*Figure 3F,3G*) revealed diminished intracellular lipid particles and cholesterol content in ox-LDL-induced VSMCs after *SRC* silencing or genistein treatment. The decline of intracellular lipid particles and cholesterol content in ox-LDL-induced VSMCs triggered by genistein was undermined by overexpressing *SRC*.

In conclusion, genistein could downregulate *SRC* to restrict ox-LDL-induced VSMC proliferation, migration,

and foaming.

Genistein repressed L-Ca channel currents by downregulate *SRC* in ox-LDL-induced VSMCs

Existing research has documented that *SRC* activates L-Ca channels (15). The results of patch-clamp experiments (*Figure 4A*) showed that cellular L-Ca channel currents were substantially decreased in ox-LDL-induced VSMCs after silencing *SRC*. Therefore, we speculate that genistein reduced L-Ca channel currents via *SRC* downregulation. After genistein treatment and *SRC* overexpression, patch-clamp experiments (*Figure 4B*) manifested conspicuous diminishment of cellular L-Ca channel currents in ox-LDL-induced VSMCs following genistein treatment, which was nullified by further overexpressing *SRC*.

In summary, genistein could curtail L-Ca channel currents by reducing *SRC* activity.
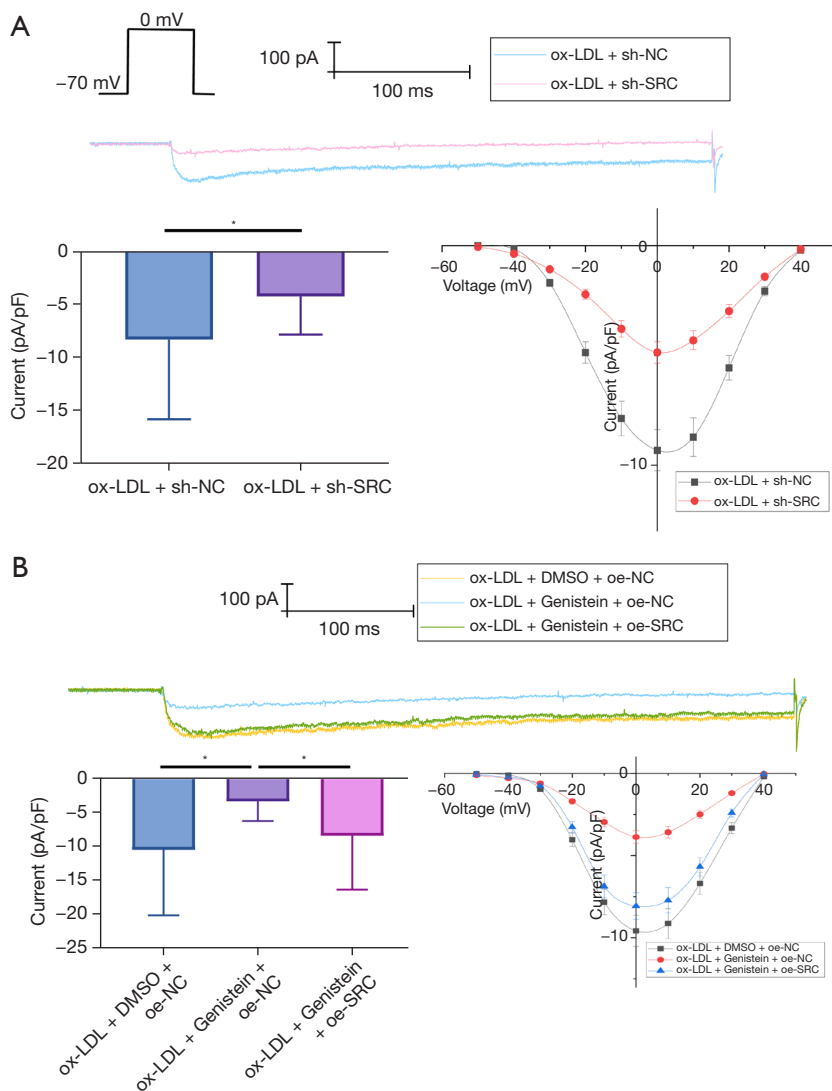
Figure 4 Genistein-mediated downregulation of *SRC* suppresses L-Ca channel currents in ox-LDL-induced VSMCs. (A) L-Ca channel currents in ox-LDL-induced VSMCs after silencing *SRC* examined by patch-clamp experiments. (B) L-Ca channel currents in ox-LDL-induced VSMCs after treatment with genistein and/or oe-*SRC* examined by Patch-clamp experiments. *P<0.05. The cell experiments were repeated 3 times independently. ox-LDL, oxidized low-density lipoprotein; VSMC, vascular smooth muscle cell; DMSO, dimethyl sulfoxide.

SRC facilitated ox-LDL-induced proliferation, migration, and foaming of VSMCs by acting on the L-Ca channel subunit CACNA1C

As a subunit of the L-Ca channel, *CACNA1C* has been reported to be involved in the process of AS (17,23). Hence, a hypothesis was proposed that *SRC* might act on *CACNA1C*. Based on western blot analysis results (*Figure 5A,5B*), AS modeling conspicuously augmented *CACNA1C* protein expression in aortic tissues of rats. In

VSMCs, ox-LDL induction evidently increased *CACNA1C* protein expression, which was neutralized by additional *SRC* silencing. The aforesaid results indicated that *CACNA1C* was highly expressed in atherosclerotic tissues of rats, and that silencing *SRC* could lower *CACNA1C* protein expression in ox-LDL-induced VSMCs.

To evaluate whether *SRC* affected the activities of ox-LDL-induced VSMCs via *CACNA1C*, *SRC* was overexpressed and *CACNA1C* was silenced in ox-LDL-
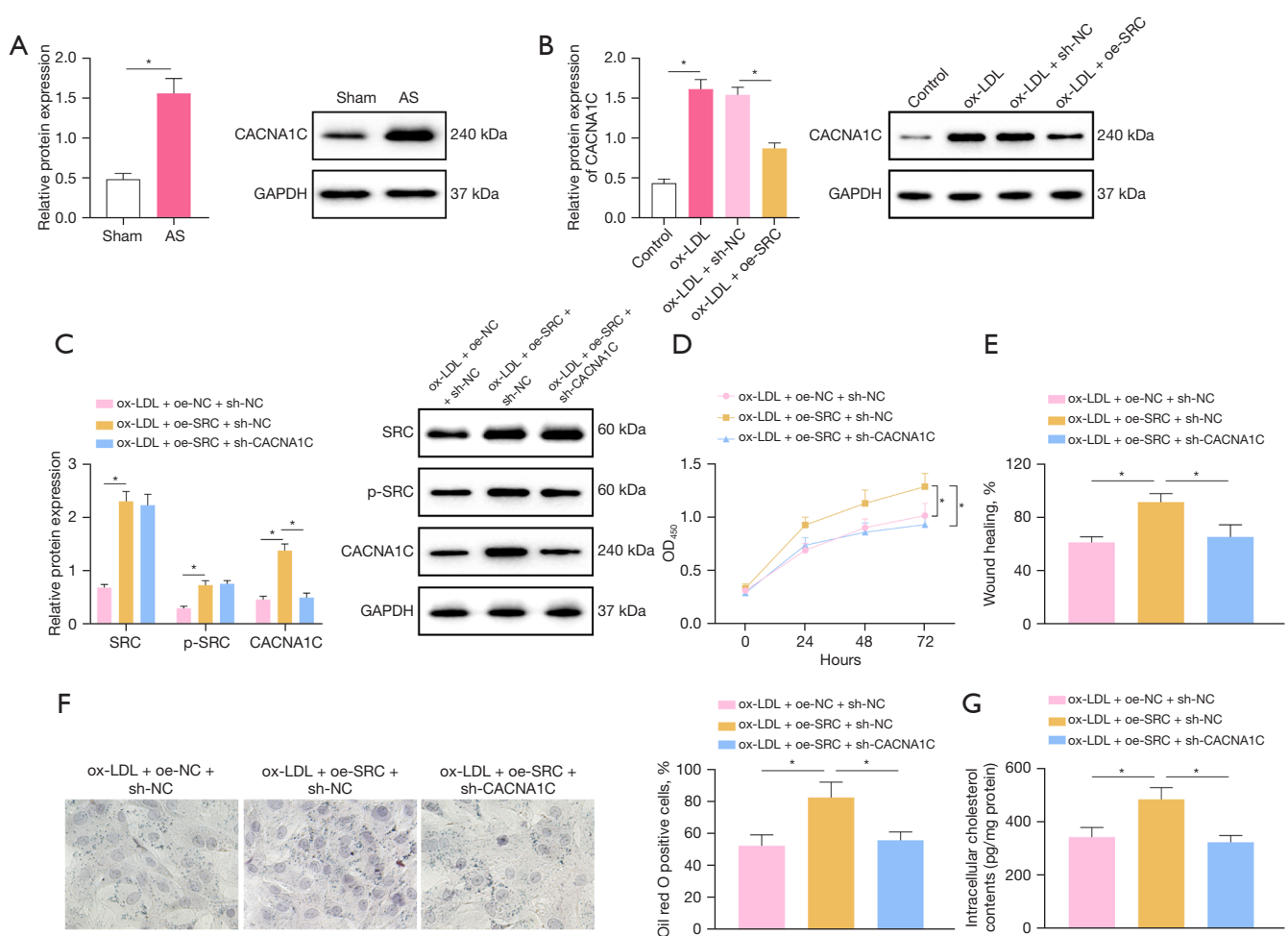
Figure 5 *SRC* upregulation acts on *CACNA1C* to promote ox-LDL-induced proliferation, migration, and foaming of VSMCs. (A) Western blot analysis of *CACNA1C* protein expression in aortic tissue of rats after AS modeling (8 rats per group). (B) Western blot analysis of *CACNA1C* protein expression in ox-LDL-induced VSMCs after silencing *SRC*. (C) Western blot analysis of *CACNA1C* protein expression in ox-LDL-induced VSMCs in response to oe-*SRC* alone or combined with sh-*CACNA1C*. (D) CCK-8 to detect viability of ox-LDL-induced VSMCs in response to oe-*SRC* alone or combined with sh-*CACNA1C*. (E) Scratch test to assess migration of ox-LDL-induced VSMCs in response to oe-*SRC* alone or combined with sh-*CACNA1C*. (F) Oil Red O staining to determine lipid deposition of ox-LDL-induced VSMCs in response to oe-*SRC* alone or combined with sh-*CACNA1C* (all observed at 200 μm). (G) Enzymatic colorimetry to measure the cholesterol content of ox-LDL-induced VSMCs in response to oe-*SRC* alone or combined with sh-*CACNA1C*. *P<0.05. The cell experiments were repeated three times independently. AS, atherosclerosis; ox-LDL, oxidized low-density lipoprotein; VSMC, vascular smooth muscle cell; DMSO, dimethyl sulfoxide; CCK-8, Cell Counting Kit-8.

induced VSMCs. As indicated by western blot analysis results (*Figure 5C*), *SRC* and *CACNA1C* protein expression were signally elevated in ox-LDL-induced VSMCs following overexpression of *SRC*, and *CACNA1C* protein expression considerably decreased in ox-LDL-induced VSMCs after silencing *CACNA1C* in the presence of *SRC* overexpression. For the results of CCK-8 and scratch test

(*Figure 5D,5E*, Figure S1D), the noticeable increase of cell proliferation and migration was observed in ox-LDL-induced VSMCs subsequent to *SRC* overexpression, whilst these trends were abolished by further silencing *CACNA1C*. Oil Red O staining and enzymatic colorimetry results (*Figure 5F,5G*) demonstrated that *SRC* overexpression caused the prominent elevation of intracellular lipid particles and

cholesterol content, which was counteracted after further silencing *CACNA1C*.

Taken together, *SRC* could accelerate the proliferation, migration, and foaming of ox-LDL-induced VSMCs by acting on the L-Ca channel subunit *CACNA1C*.

Silencing CACNA1C restricted ox-LDL-induced proliferation, migration, and foaming of VSMCs through downregulation of LOX-1

Existing literature has demonstrated that *CACNA1C* facilitates cellular uptake of ox-LDL by upregulating *LOX-1* (18). Western blot analysis (*Figure 6A,6B*) exhibited that *LOX-1* protein expression was evidently elevated in aortic tissues of rats after AS modeling and in VSMCs following ox-LDL induction. In ox-LDL-exposed VSMCs, *LOX-1* protein expression considerably diminished after silencing *CACNA1C*, which was annulled by further overexpression of *LOX-1*. The data revealed that *LOX-1* expression was high in atherosclerotic tissues of rats and that silencing *CACNA1C* resulted in downregulation of *LOX-1*.

Immunofluorescence (*Figure 6C*) manifested that *CACNA1C* silencing prominently lowered cellular uptake of Dil-ox-LDL by VSMCs, which was negated after additional *LOX-1* overexpression. The results of CCK-8 and scratch test (*Figure 6D,6E*, Figure S1E) displayed the marked reduction of ox-LDL-exposed VSMC proliferation and migration after silencing of *CACNA1C*, which was counteracted following further overexpression of *LOX-1*. The results of Oil Red O staining and enzymatic colorimetry (*Figure 6F,6G*) depicted that *CACNA1C* silencing appreciably decreased intracellular lipid particles and cholesterol content in ox-LDL-exposed VSMCs and that additional *LOX-1* overexpression abrogated these trends.

In summary, *CACNA1C* silencing reduced the uptake of ox-LDL by VSMCs by downregulating *LOX-1*, thereby repressing ox-LDL-induced proliferation, migration, and foaming of VSMCs.

Overexpression of LOX-1 counterweighed the ameliorative impacts of genistein on AS in rats and ox-LDL on VSMCs

To further elucidate the mechanism by which genistein alleviated AS in vivo, AS rats were treated with genistein and oe-*LOX-1*. Western blot analysis (*Figure 7A*) manifested that genistein treatment of AS rats strikingly lowered *SRC* phosphorylation level and *CACNA1C* and
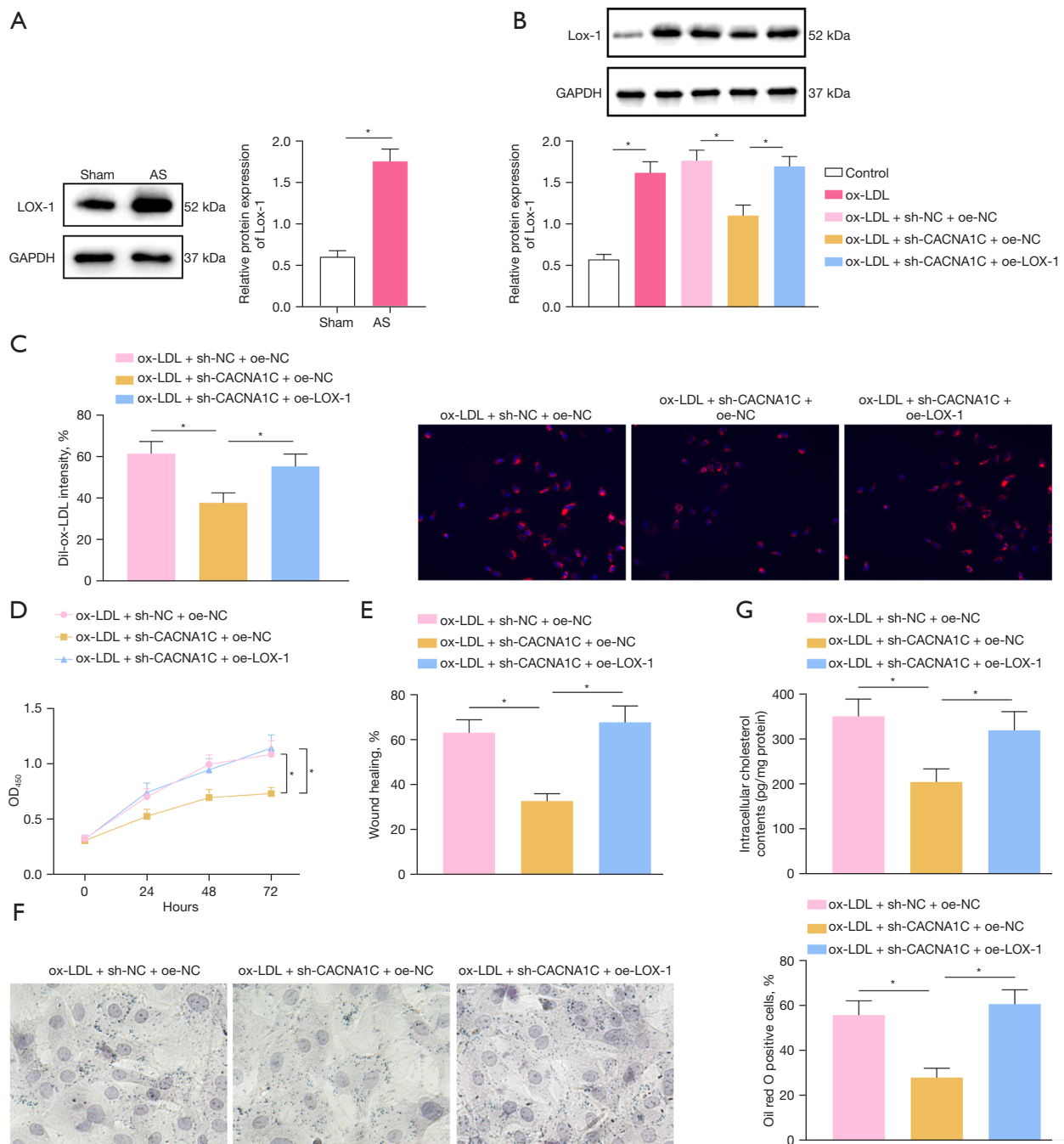
LOX-1 protein expression in aortic tissues. Meanwhile, *LOX-1* overexpression reversed the decrease of *LOX-1* protein expression triggered by genistein without impacts on *SRC* phosphorylation level and *CACNA1C* protein expression. As illustrated by the results Oil Red O staining and HE staining (*Figure 7B-7D*), observably decreased atherosclerotic plaque lesion areas and lipid deposition were found in AS rats after genistein treatment, which was neutralized by additional overexpression of *LOX-1*.

The ox-LDL-exposed VSMCs were treated with genistein and oe-*LOX-1*. Western blot analysis (*Figure 7E*) showed that genistein treatment dramatically lowered *SRC* phosphorylation level and *CACNA1C* and *LOX-1* protein expression in ox-LDL-exposed VSMCs. In the presence of genistein, overexpression of *LOX-1* augmented *LOX-1* protein expression but did not affect *SRC* phosphorylation level and *CACNA1C* protein expression in ox-LDL-exposed VSMCs. For immunofluorescence results (*Figure 7F*), cellular uptake of Dil-ox-LDL by VSMCs was observably reduced after genistein treatment, which was noticeably nullified through further overexpression of *LOX-1*. The CCK-8 and scratch test results demonstrated that ox-LDL-exposed VSMC proliferation and migration were markedly diminished following genistein treatment, which was abrogated after additional *LOX-1* overexpression (*Figure 7G,7H*, Figure S1F). Oil Red O staining and enzymatic colorimetry showed the diminishment in intracellular lipid particles and cholesterol content inox-LDL-exposed VSMC after genistein treatment and that these results were negated by further overexpressing *LOX-1* (*Figure 7I,7J*).

Together, *LOX-1* upregulation abolished the alleviatory impacts of genistein on AS in rats and ox-LDL on VSMCs.

Discussion

Genistein supplementation is an attractive alternative for cardiovascular protection based on previous epidemiological and animal model studies (24). The study of Thangavel *et al.* has highlighted inhibitory effect of genistein on incidence of cardiovascular disease, osteoporosis, and the postmenopausal symptoms (25). Some ideas have been presented by Si *et al.* demonstrating the possible mechanisms of the genistein action on vascular protective effects, where genistein may attenuate pro-inflammatory factor-induced vascular endothelial barrier dysfunction, inactivate the cAMP/PKA cascade, activate peroxisome proliferator-activated receptors, or reduce production of reactive oxygen

Figure 6 *CACNA1C* silencing diminishes *LOX-1* expression to restrain the proliferation, migration, and foaming of ox-LDL-exposed VSMCs. (A) Western blot analysis to measure *LOX-1* protein expression in aortic tissue of rats after AS modeling (8 rats per group). (B) Western blot analysis of *LOX-1* protein expression in ox-LDL-exposed VSMCs after *CACNA1C* silencing and *LOX-1* overexpression. ox-LDL-induced VSMCs were treated with sh-NC + oe-NC, sh-*CACNA1C* + oe-NC, or sh-*CACNA1C* + oe-*LOX-1*. (C) Immunofluorescence to assess the uptake of Dil-ox-LDL by VSMCs (all observed at 100 μm). (D) VSMC viability determined by CCK-8. (E) VSMC migration examined by scratch test. (F) Lipid deposition in VSMCs analyzed by Oil Red O staining (all observed at 200 μm). (G) Cholesterol content in VSMCs observed by enzymatic colorimetry. *P<0.05. The cell experiments were repeated 3 times independently. LOX-1, lectin-like oxidized LDL receptor-1; ox-LDL, oxidized low-density lipoprotein; AS, atherosclerosis; VSMC, vascular smooth muscle cell; DMSO, dimethyl sulfoxide; CCK-8, Cell Counting Kit-8.
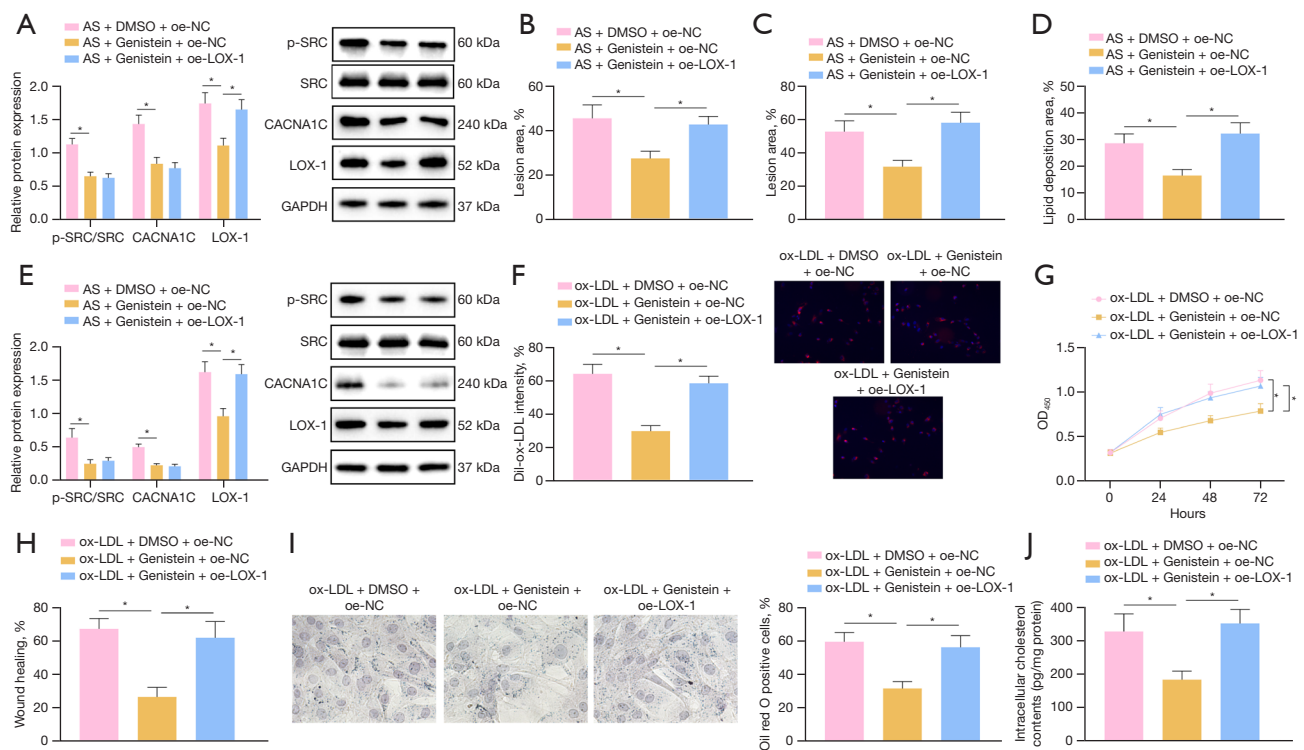
Figure 7 The attenuating effects of genistein on AS *in vivo* and ox-LDL *in vitro* are annulled through upregulation of *LOX-1*. AS rats were treated with DMSO + oe-NC, genistein + oe-NC, or genistein + oe-*LOX-1*. (A) Western blot analysis of *SRC* phosphorylation level and *CACNA1C* and *LOX-1* protein expression in aortic tissue of rats (8 rats per group). (B) Oil Red O staining analysis of whole aortic atherosclerotic lesion areas (8 rats per group). (C) HE staining observation of aortic root lesion areas (8 rats per group). (D) Oil Red O staining to measure the percentage of aortic root lipids (8 rats per group). The ox-LDL-exposed VSMCs were treated with DMSO + oe-NC, genistein + oe-NC, or genistein + oe-*LOX-1*. (E) *SRC* phosphorylation level and *CACNA1C* and *LOX-1* protein expression in VSMCs determined by Western blot analysis. (F) The uptake of Dil-ox-LDL by VSMCs assessed by immunofluorescence (all observed at 100 μm). (G) CCK-8 to evaluate VSMC viability. (H) Scratch test to examine VSMC migration. (I) Oil Red O staining to observe lipid deposition in VSMCs (all observed at 200 μm). (J) Enzymatic colorimetry to determine cholesterol content in VSMCs. *$P<0.05$. The cell experiments were repeated 3 times independently. AS, atherosclerosis; LOX-1, lectin-like oxidized LDL receptor-1; ox-LDL, oxidized low-density lipoprotein; VSMC, vascular smooth muscle cell; DMSO, dimethyl sulfoxide; CCK-8, Cell Counting Kit-8; HE, hematoxylin and eosin.

species-producing enzymes (26). However, few studies exist to provide a clear mechanistic understanding of the molecular mechanistic basis of genistein in AS. Based on this, this research set out to ascertain the mechanism of genistein in AS, and the obtained data revealed that genistein might reduce the uptake of ox-LDL by VSMCs through inhibiting *SRC* action on the L-Ca channel subunit *CACNA1C* to downregulate *LOX-1*, thereby suppressing ox-LDL-induced proliferation, migration, and foaming of VSMCs and preventing the formation of AS (*Figure 8*).

The initial finding in our research was that genistein alleviated AS in rats. Similarly, mounting evidence has illustrated the atheroprotective impacts of genistein. For

instance, it has been displayed that genistein can repress tumor necrosis factor-α (TNF-α)-triggered adhesion of monocytes to human umbilical vein endothelial cells, a crucial event in AS pathogenesis (27). In addition, a prior work had indicated that a genistein derivative, 7-Difluoromethyl-5,4'-dimethoxygenistein, can lower lipid plasma levels to curtail AS development (28). On the grounds of 'inflammation' hypotheses of AS formation, anti-inflammatory agents hold remarkable potential for AS management (29). Of interest, genistein has been suggested to present anti-inflammatory properties in VSMCs of atherosclerosis lesions, which were realized by regulating the ER-p38/ERK1/2-PPARγ-NF-κB-CRP/MMP-9 axis (30).
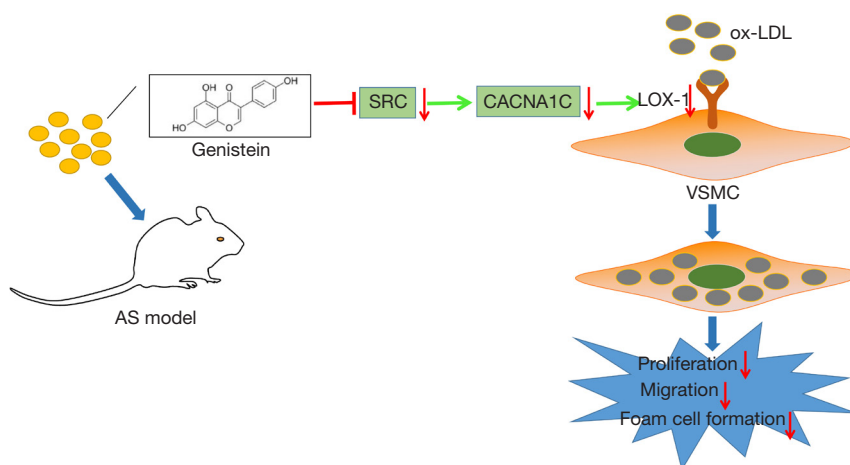
Figure 8 The mechanism graph of genistein in AS. Genistein inhibits the uptake of ox-LDL by VSMCs by restricting *SRC* action on the L-Ca channel subunit *CACNA1C* to downregulate *LOX-1*, thus decreasing ox-LDL-induced proliferation, migration, and foaming of VSMCs and preventing the formation of AS. AS, atherosclerosis; ox-LDL, oxidized low-density lipoprotein; VSMC, vascular smooth muscle cell; LOX-1, lectin-like oxidized LDL receptor-1.

Moreover, another study revealed that genistein causes significant declines in the formation of atherosclerotic plaques in LDL receptor-/- rats by downregulating inflammatory NF-kB and VCAM-1 (31).It should be noted that VSMCs are a primary cell type existing at all stages of atherosclerotic plaques (32).

In the subsequent assays, we observed that genistein diminished VSMC proliferation, migration, and foaming caused by ox-LDL. Consistent with our results, the research performed by Bai *et al.* elucidated that genistein restricted the proliferation of ox-LDL-induced VSMCs (11). Besides, a prior work unraveled that genistein resulted in the decrease in VSMC proliferation and migration during neointima formation (33). Genistein could suppress VSMC-derived foam cell formation through the downregulation of *LOX-1* by blocking tyrosine kinase pathway (34). Furthermore, our work exhibited that inhibition of L-Ca channels participated in the suppressive impacts of genistein on ox-LDL-induced VSMC proliferation, migration, and foaming. Concordant with our findings, it was noted in a previous study that genistein restrained L-Ca channels in gastrointestinal smooth muscle (35). Of note, the L-Ca channel blocker, diltiazem, has been documented to reduce VSMC migration during AS (36). Also, it was previously reported that another L-Ca channel blocker, nifedipine, exerted anti-proliferative effects on rat aortic VSMCs (37), which is in line with our results. Hence, genistein suppressed L-Ca channels to diminish ox-LDL-induced

VSMC proliferation, migration, and foaming.

Another finding of our study was that genistein restricted ox-LDL-induced VSMC proliferation, migration, and foaming by inhibiting *SRC* activity. This finding is partially supported by a report by Lee *et al.* that genistein obviously decreased *SRC* phosphorylation in prostate cancer cells (38). A recent report unveiled that repressing *SRC* activation attenuated ox-LDL-induced lipid accumulation and foam cell formation in VSMCs (39). Concordantly, Lang *et al.* demonstrated that the downregulation of *SRC* correlated to the reduced proliferation and migration of hydrogen peroxide-exposed VSMCs (40). Notably, another study manifested that c-*SRC* could induce the migration of VSMCs through activating L-Ca channels (8), which is in parallel with our results that genistein suppressed L-Ca channels by reducing *SRC* activity.

Besides, we observed that *SRC* accelerated ox-LDL-triggered proliferation, migration, and foaming of VSMCs via *LOX-1* downregulation by acting on *CACNA1C*. As an L-Ca channel subunit (23), *CACNA1C* has been implicated in AS formation (17). Moreover, the same relationship between *CACNA1C* and *LOX-1* was illustrated in a previous study (18). More importantly, the anti-atherosclerotic activity of *LOX-1* has been found by the research of Li *et al.* (41). Concurrently, a recent work exhibited that *LOX-1* overexpression was associated with VSMC proliferation caused by ox-LDL (42). As previously reported, *LOX-1* downregulation culminated in restricted ox-LDL-exposed

foam cell formation in rat aortic VSMCs, thus exerting an ameliorating effect in AS formation (43,44). In alignment with our findings, *LOX-1* upregulation was involved in ox-LDL-triggered VSMC proliferation, migration, and foam cell formation (45).

Taken together, our study adds to the growing evidence for the atheroprotective effects of genistein. Specifically, genistein protected VSMCs against ox-LDL-exposed proliferation, migration, and foam cell formation through *LOX-1* downregulation by blocking the action of *SRC* on the L-Ca channel subunit *CACNA1C*, which alleviated AS. Investigation of genistein and the *SRC/CACNA1C/LOX-1* axis in VSMCs and AS yields a better understanding of their *in vivo* mechanisms and may have potentially critical therapeutic implications in the treatment of AS.

Acknowledgments

Footnote

Reporting Checklist: The authors have completed the ARRIVE reporting checklist. Available at https://atm.amegroups.com/article/view/10.21037/atm-22-2113/rc

Data Sharing Statement: Available at https://atm.amegroups.com/article/view/10.21037/atm-22-2113/dss

Conflicts of Interest: All authors have completed the ICMJE uniform disclosure form (available at https://atm.amegroups.com/article/view/10.21037/atm-22-2113/coif). The authors have no conflicts of interest to declare.

Ethical Statement: The authors are accountable for all aspects of the work in ensuring that questions related to the accuracy or integrity of any part of the work are appropriately investigated and resolved. Animal experiments were performed under a project license (No. 2021086) granted by Animal Ethical Care Committee of the First Affiliated Hospital of Harbin Medical University, in compliance with institutional guidelines for the care and use of animals.

Open Access Statement: This is an Open Access article distributed in accordance with the Creative Commons Attribution-NonCommercial-NoDerivs 4.0 International

References

1. Kobiyama K, Ley K. Atherosclerosis. Circ Res 2018;123:1118-20.

2. Libby P. The changing landscape of atherosclerosis. Nature 2021;592:524-33.

3. Frostegård J. Immunity, atherosclerosis and cardiovascular disease. BMC Med 2013;11:117.

4. Zhu Y, Xian X, Wang Z, et al. Research Progress on the Relationship between Atherosclerosis and Inflammation. Biomolecules 2018;8:80.

5. Chistiakov DA, Melnichenko AA, Myasoedova VA, et al. Mechanisms of foam cell formation in atherosclerosis. J Mol Med (Berl) 2017;95:1153-65.

6. Wang Z, Guo X, Zhang Q, et al. Elimination of Ox-LDL through the liver inhibits advanced atherosclerotic plaque progression. Int J Med Sci 2021;18:3652-64.

7. Pryma CS, Ortega C, Dubland JA, et al. Pathways of smooth muscle foam cell formation in atherosclerosis. Curr Opin Lipidol 2019;30:117-24.

8. Guo X, Kashihara T, Nakada T, et al. PDGF-induced migration of synthetic vascular smooth muscle cells through c-Src-activated L-type Ca2+ channels with full-length CaV1.2 C-terminus. Pflugers Arch 2018;470:909-21.

9. Mukund V, Mukund D, Sharma V, et al. Genistein: Its role in metabolic diseases and cancer. Crit Rev Oncol Hematol 2017;119:13-22.

10. Wei J, Yao Z, Li H, et al. Genistein alleviates atherosclerosis in apolipoprotein E-deficient mice by interrupting the OX40/OX40L pathway. Int J Clin Exp Pathol 2019;12:1658-65.

11. Bai B, Lu N, Zhang W, et al. Inhibitory Effects of Genistein on Vascular Smooth Muscle Cell Proliferation Induced by Ox-LDL: Role of BKCa Channels. Anal Cell Pathol (Amst) 2020;2020:8895449.

12. Ono M, Takeshima M, Nishi A, et al. Genistein Suppresses v-Src-Driven Proliferative Activity by Arresting the Cell-Cycle at G2/M through Increasing p21 Level in Src-Activated Human Gallbladder Carcinoma cells. Nutr Cancer 2021;73:1471-9.

13. Bagnato G, Leopizzi M, Urciuoli E, et al. Nuclear

Functions of the Tyrosine Kinase Src. Int J Mol Sci 2020;21:2675.

14. Wang JG, Aikawa M. Toll-like receptors and Src-family kinases in atherosclerosis -- focus on macrophages. Circ J 2015;79:2332-4.

15. Kashihara T, Nakada T, Kojima K, et al. Angiotensin II activates CaV 1.2 Ca2+ channels through β-arrestin2 and casein kinase 2 in mouse immature cardiomyocytes. J Physiol 2017;595:4207-25.

16. Kabir ZD, Martínez-Rivera A, Rajadhyaksha AM. From Gene to Behavior: L-Type Calcium Channel Mechanisms Underlying Neuropsychiatric Symptoms. Neurotherapeutics 2017;14:588-613.

17. Peng C, Ding Y, Yi X, et al. Association study of CACNA1C polymorphisms with large artery atherosclerotic stroke in Chinese Han population. Neurol Res 2018;40:677-82.

18. Komoda H, Shiraki A, Oyama JI, et al. Azelnidipine Inhibits the Differentiation and Activation of THP-1 Macrophages through the L-Type Calcium Channel. J Atheroscler Thromb 2018;25:690-7.

19. Cheng XL, Ding F, Wang DP, et al. Hexarelin attenuates atherosclerosis via inhibiting LOX-1-NF-κB signaling pathway-mediated macrophage ox-LDL uptake in ApoE-/- mice. Peptides 2019;121:170122.

20. Yu XH, Chen JJ, Deng WY, et al. Biochanin A Mitigates Atherosclerosis by Inhibiting Lipid Accumulation and Inflammatory Response. Oxid Med Cell Longev 2020;2020:8965047.

21. Belevych AE, Warrier S, Harvey RD. Genistein inhibits cardiac L-type Ca(2+) channel activity by a tyrosine kinase-independent mechanism. Mol Pharmacol 2002;62:554-65.

22. Yin C, Vrieze AM, Rosoga M, et al. Efferocytic Defects in Early Atherosclerosis Are Driven by GATA2 Overexpression in Macrophages. Front Immunol 2020;11:594136.

23. Hedley PL, Jørgensen P, Schlamowitz S, et al. The genetic basis of Brugada syndrome: a mutation update. Hum Mutat 2009;30:1256-66.

24. Dixon RA, Ferreira D. Genistein. Phytochemistry 2002;60:205-11.

25. Thangavel P, Puga-Olguín A, Rodríguez-Landa JF, et al. Genistein as Potential Therapeutic Candidate for Menopausal Symptoms and Other Related Diseases. Molecules 2019;24:3892.

26. Si H, Liu D. Phytochemical genistein in the regulation of vascular function: new insights. Curr Med Chem 2007;14:2581-9.

27. Jia Z, Babu PV, Si H, et al. Genistein inhibits TNF-α-induced endothelial inflammation through the protein kinase pathway A and improves vascular inflammation in C57BL/6 mice. Int J Cardiol 2013;168:2637-45.

28. Zhang Y, Li L, You J, et al. Effect of 7-difluoromethyl-5, 4'-dimethoxygenistein on aorta atherosclerosis in hyperlipidemia ApoE(-/-) mice induced by a cholesterol-rich diet. Drug Des Devel Ther 2013;7:233-42.

29. Xu S, Pelisek J, Jin ZG. Atherosclerosis Is an Epigenetic Disease. Trends Endocrinol Metab 2018;29:739-42.

30. Xu L, Liu JT, Li K, et al. Genistein inhibits Ang II-induced CRP and MMP-9 generations via the ER-p38/ERK1/2-PPARγ-NF-κB signaling pathway in rat vascular smooth muscle cells. Life Sci 2019;216:140-6.

31. Wang J, Zhang R, Xu Y, et al. Genistein inhibits the development of atherosclerosis via inhibiting NF-kappaB and VCAM-1 expression in LDLR knockout mice. Can J Physiol Pharmacol 2008;86:777-84.

32. Basatemur GL, Jørgensen HF, Clarke MCH, et al. Vascular smooth muscle cells in atherosclerosis. Nat Rev Cardiol 2019;16:727-44.

33. Tsai YC, Leu SY, Peng YJ, et al. Genistein suppresses leptin-induced proliferation and migration of vascular smooth muscle cells and neointima formation. J Cell Mol Med 2017;21:422-31.

34. Lin J, Xu Y, Zhao T, et al. Genistein suppresses smooth muscle cell-derived foam cell formation through tyrosine kinase pathway. Biochem Biophys Res Commun 2015;463:1297-304.

35. Zhang LX, Li HF, Wang LD, et al. Resveratrol and genistein inhibition of rat isolated gastrointestinal contractions and related mechanisms. World J Gastroenterol 2014;20:15335-42.

36. Liu W, Hashimoto T, Yamashita T, et al. Coagulation factor XI induces Ca2+ response and accelerates cell migration in vascular smooth muscle cells via proteinase-activated receptor 1. Am J Physiol Cell Physiol 2019;316:C377-92.

37. Sung JY, Choi HC. Nifedipine inhibits vascular smooth muscle cell proliferation and reactive oxygen species production through AMP-activated protein kinase signaling pathway. Vascul Pharmacol 2012;56:1-8.

38. Lee J, Ju J, Park S, et al. Inhibition of IGF-1 signaling by genistein: modulation of E-cadherin expression and downregulation of β-catenin signaling in hormone refractory PC-3 prostate cancer cells. Nutr Cancer 2012;64:153-62.

39. Chen Z, Xue Q, Cao L, et al. Toll-Like Receptor 4

Mediated Oxidized Low-Density Lipoprotein-Induced Foam Cell Formation in Vascular Smooth Muscle Cells via Src and Sirt1/3 Pathway. Mediators Inflamm 2021;2021:6639252.

40. Lang Y, Chen D, Li D, et al. Luteolin inhibited hydrogen peroxide-induced vascular smooth muscle cells proliferation and migration by suppressing the Src and Akt signalling pathways. J Pharm Pharmacol 2012;64:597-603.

41. Li Q, Zhao W, Zeng X, et al. Ursolic Acid Attenuates Atherosclerosis in ApoE-/- Mice: Role of LOX-1 Mediated by ROS/NF-κB Pathway. Molecules 2018;23:1101.

42. Zhang Z, Zhang D, Du B, et al. Hyperoside inhibits the effects induced by oxidized low-density lipoprotein in vascular smooth muscle cells via oxLDL-LOX-1-ERK pathway. Mol Cell Biochem 2017;433:169-76.

43. Cheng CI, Tai MH, Chang HR, et al. Oxidized low-density lipoprotein induced hepatoma-derived growth factor upregulation mediates foam cell formation of cultured rat aortic vascular smooth muscle cells. Eur J Cell Biol 2021;100:151169.

44. Zhang D, Gao JL, Zhao CY, et al. Cyclin G2 promotes the formation of smooth muscle cells derived foam cells in atherosclerosis via PP2A/NF-κB/LOX-1 pathway. Ann Transl Med 2021;9:446.

45. Li W, Zhi W, Zhao J, et al. Cinnamaldehyde protects VSMCs against ox-LDL-induced proliferation and migration through S arrest and inhibition of p38, JNK/MAPKs and NF-κB. Vascul Pharmacol 2018;108:57-66.

(English Language Editor: J. Jones)

A

| Control | ox-LDL | ox-LDL + DMSO | ox-LDL + Genistein |

B

| ox-LDL + DMSO | ox-LDL + Genistein | ox-LDL + BayK8644 | ox-LDL + Nifedipine | ox-LDL + Genistein + BayK8644 |

C

| ox-LDL + sh-NC | ox-LDL + sh-SRC | ox-LDL + DMSO + oe-NC | ox-LDL + Genistein + oe-NC | ox-LDL + Genistein + oe-SRC |

D

| ox-LDL + oe-NC + sh-NC | ox-LDL + oe-SRC + sh-NC | ox-LDL + oe-SRC + sh-CACNA1C |

E

| ox-LDL + sh-NC + oe-NC | ox-LDL + sh-CACNA1C + oe-NC | ox-LDL + sh-CACNA1C + oe-Lox-1 |

F

| ox-LDL + DMSO + oe-NC | ox-LDL + Genistein + oe-NC | ox-LDL + Genistein + oe-Lox-1 |

Figure S1 Representative images of scratch tests for quantification of VSMC migration in panels 1F (A), 2D (B), 3E (C), 5E (D), 6E (E), and 7H (F) (observed at 200 µm and photographed under an inverted microscope).